

their complexity offers interesting properties: Parafermionic chains can simultaneously host symmetry breaking and non-trivial topology [11, 12]; moreover, parafermionic zero-energy edge modes can be of different nature [13] ("strong" or "weak" depending on whether they extend to the full spectrum or to the low-energy manifold only).

In parallel with this plethora of parafermionic phases, quantum clock models can host a wider variety of phases compared to the Ising model. Already the simplest case with $q = 3$ shows, in addition to the trivial and the symmetry-breaking phase, also a gapless incommensurate phase [4]. In the incommensurate phase correlations decay algebraically and are characterized by a wavelength that is incommensurate with the lattice spacing. This rich phase diagram depends on an additional parameter, the chirality, i.e. the explicit breaking of charge conjugation symmetry [2, 14, 15, 16], which is not present in the \mathbb{Z}_2 case. Very little is known on the phase diagrams and the phase transitions of clock models with $q > 3$: for example, for $q \geq 5$ the self-dual clock models exhibit phase transitions of the Kosterlitz-Thouless universality class [17, 3, 7]. In general, characterizing the phase transitions of clock models has required a considerable theoretical effort and the application of advanced numerical techniques [4, 5, 6, 18, 19].

Quantum clock models are interesting also from the point of view of experiments and applications. In a recent experiment with Rydberg atom chains [20] it has been observed that Rydberg excitations on the chains can arrange in \mathbb{Z}_q ordered states, with phase transitions belonging to the same universality class as \mathbb{Z}_q clocks. Furthermore, clock models could be used for realizing exotic phases of matter, such as many-body localized phases and Floquet time crystals with arbitrary period n -tupling [21, 22]: time-translation symmetry breaking can occur in disordered one-dimensional short-range clock models, but also in models with infinite-range interactions.

In this paper we inquire in more depth and generality the nature of phase transitions in the clock models with infinite-range interactions. We use a mean-field analysis which in this context is exact in the thermodynamic limit and allows us to directly study the properties of the order parameter, while numerical works in one dimension focused on other probes for the transition, like the entanglement entropy [4], the ground-state degeneracy or the fidelity susceptibility [7]. The model we study is a generalization of the p -spin model [23, 24, 25] (with $p = 1$ corresponding to the case of two-body interactions). We allow for an explicit breaking of charge conjugation symmetry, parameterized by the phase φ . We find that the phase structure is simpler than the one of the one-dimensional short-range model: there are a disordered phase and a broken-symmetry phase, and the transition between the two phases is either first or second order depending on q and p . We reconstruct the phase diagram in all the cases, by finding the transition point as a function of the chirality φ .

The paper is organized as follows. In Section 2 we introduce the Hamiltonian and discuss its symmetries. In Section 3 we derive the free energy density by mean-field treatment and we discuss the possible phase transitions in the light of the symmetries. In Section 4 we compare the numerical results concerning the continuous phase transition with the analytical results obtained via perturbation theory. We are able to derive the analytical expression of the phase-boundary line (see Fig. 2) for $q \geq 4$. In Section 5 we discuss the fully chiral case $\varphi = \pi/q$ and we interpret the corresponding absence of the trivial phase as an exception to the analytic expansion of the free energy density introduced in Section 2. In Section 6 we consider the limit of large q and study its thermodynamic properties using a harmonic approximation. We conclude and present the perspectives of future work in Section 7. In all the paper we will assume the Planck constant $\hbar = 1$ and the Boltzmann constant $k_B = 1$.

2. The model

In this section we introduce the \mathbb{Z}_q -invariant fully connected model (Sec. 2.1). We summarize the phase structure of our model in Sec. 2.2.

2.1. Hilbert space and Hamiltonian

Clock models generalize the Ising \mathbb{Z}_2 symmetry to a symmetry \mathbb{Z}_q with an integer $q \geq 2$ [8]. We consider a system of N clock variables: each variable has q possible states, that can be pictorially represented as q points on a unit circle (see Fig. 1). We label each state with the corresponding complex number,

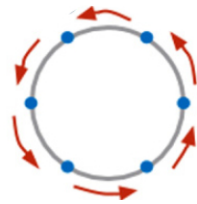


Figure 1. Pictorial representation of a clock variable with $q = 6$. It belongs to a q -dimensional Hilbert space, and the blue points on the circle indicate the possible states of the clock in the basis where σ is diagonal. The red arrows represent the action of the τ operators in this basis.

which can assume the values $1, \omega, \omega^2, \dots, \omega^{q-1}$, where $\omega = e^{2\pi i/q}$. On the q -dimensional Hilbert space of a quantum clock variable we define the two operators $\hat{\sigma}$ and $\hat{\tau}$ that generalize the Pauli matrices $\hat{\sigma}^z, \hat{\sigma}^x$. They satisfy

$$\hat{\sigma}^q = \hat{\tau}^q = 1, \quad \hat{\sigma}^\dagger = \hat{\sigma}^{q-1}, \quad \hat{\tau}^\dagger = \hat{\tau}^{q-1}, \quad (1)$$

$$\hat{\sigma}\hat{\tau} = \omega\hat{\tau}\hat{\sigma}. \quad (2)$$

A convenient representation for the operators is the following

$$\hat{\sigma} = \begin{pmatrix} 1 & 0 & 0 & \dots & 0 \\ 0 & \omega & 0 & \dots & 0 \\ 0 & 0 & \omega^2 & \dots & 0 \\ \vdots & \vdots & \vdots & \dots & \vdots \\ 0 & 0 & 0 & \dots & \omega^{q-1} \end{pmatrix}, \quad \hat{\tau} = \begin{pmatrix} 0 & 0 & 0 & \dots & 0 & 1 \\ 1 & 0 & 0 & \dots & 0 & 0 \\ 0 & 1 & 0 & \dots & 0 & 0 \\ \vdots & \vdots & \vdots & \dots & \vdots & \vdots \\ 0 & 0 & 0 & \dots & 1 & 0 \end{pmatrix} \quad (3)$$

In this representation, $\hat{\sigma}$ measures the position on the unit circle, and $\hat{\tau}$ shifts the state of one position counter-clockwise along the circle. In the case $q = 2$, the matrices in Eq. (3) coincide with the canonical Pauli matrices $\hat{\sigma}_z, \hat{\sigma}_x$.

We define a Hamiltonian for N sites, in terms of $\hat{\sigma}_j$ and $\hat{\tau}_j$ acting on site j . On the same site the operators satisfy the relations in Eqs. (1,2), and on different sites they commute. We define the two operators

$$\hat{m}_\sigma = \frac{1}{N} \sum_{j=1}^N \hat{\sigma}_j, \quad \hat{m}_\tau = \frac{1}{N} \sum_{j=1}^N \hat{\tau}_j \quad (4)$$

which represent the total ‘‘magnetizations’’ along $\hat{\sigma}$ and $\hat{\tau}$. The Hamiltonian of our fully connected model is then defined as

$$\hat{H} = -N (\hat{m}_\sigma \hat{m}_\sigma^\dagger)^p - hq^2 N (\hat{m}_\tau e^{i\varphi} + \hat{m}_\tau^\dagger e^{-i\varphi}), \quad (5)$$

where $p \geq 1$, $h \geq 0$ is the transverse field, φ is real and the factors N guarantee the extensivity.

The case $q = 2$ and $\varphi = 0$ corresponds to the fully connected p -spin ferromagnet [23]. Before proceeding, we briefly outline the main features for this case. In the limit of large h , one observes a paramagnetic \mathbb{Z}_2 invariant state. For h below a critical value, on the opposite, the system chooses between two broken-symmetry states which physically correspond to a ferromagnet with all spins pointing either up or down in the z direction. The nature of the transition separating these two phases is second order for $p = 1$ and first order for $p > 1$. The case of $p \rightarrow \infty$ is connected to Grover’s search algorithm [26].

Qualitatively one would expect a similar behaviour in the case of $q > 2$ and $\varphi = 0$ (i.e. q broken symmetry states for $h \rightarrow 0$, and a \mathbb{Z}_q invariant para-magnetic phase for $h \rightarrow \infty$). The crux of this paper will be the elucidation of the nature of the phase transitions for $q \geq 2$ and the interesting behaviour that arises with the introduction of chirality ($\varphi \neq 0$). To this end, it is important to discuss the symmetries of the model.

The Hamiltonian (5) has a global \mathbb{Z}_q symmetry generated by the unitary operator

$$\hat{G} = \prod_{j=1}^N \hat{\tau}_j. \quad (6)$$

We can also notice that the Hamiltonian is invariant under time reversal, which is defined as the antiunitary transformation

$$\hat{T} \hat{\sigma}_j \hat{T} = \hat{\sigma}_j^\dagger, \quad \hat{T} \hat{\tau}_j \hat{T} = \hat{\tau}_j, \quad \hat{T}^2 = \mathbb{I}. \quad (7)$$

We introduce the charge conjugation unitary operator

$$\hat{C} \hat{\sigma}_j \hat{C} = \hat{\sigma}_j, \quad \hat{C} \hat{\tau}_j \hat{C} = \hat{\tau}_j^\dagger, \quad \hat{C}^2 = \mathbb{I}. \quad (8)$$

This transformation is a symmetry only for $\varphi = 0$. We refer to this special case as the non-chiral clock model, while the parameter φ is called chirality. In general, charge conjugation transforms the Hamiltonian by changing sign to the chirality: $\hat{C} \hat{H}(\varphi) \hat{C} = \hat{H}(-\varphi)$. The global operator

$$\hat{K} = \prod_{j=1}^N \hat{\sigma}_j^\dagger. \quad (9)$$

transforms the Hamiltonian as $\hat{K}^{-1} \hat{H}(\varphi) \hat{K} = \hat{H}(\varphi + 2\pi/q)$. Therefore, using the combined action of \hat{C} and \hat{K} , we can restrict without loss of generality to the case $0 \leq \varphi \leq \pi/q$.

2.2. Summary of the results

We find that the phase diagram of the model in Eq. (5) contains a trivial phase and a symmetry-breaking phase.

For $q = 3$, $p = 1$ the transition between the trivial phase and the symmetry-breaking phase is first order (we show the phase diagram in Fig. 2). The most peculiar point is at chirality $\varphi = \pi/3$: The value of the field at the transition goes to infinity as we approach $\varphi = \pi/3$, and the system is always in a broken symmetry phase for that value of φ .

For any $q > 3$, $p = 1$ in the infinite-range model there is a second-order transition from symmetry-breaking to trivial phase. We show the phase diagram for $q = 5$ in Fig. 2. The phase-boundary curve is given by the analytical formula in Eq. (18).

For $p > 1$, on the other hand, the transition is of first order for any value of q . In all these cases, when $\varphi = \pi/q$ (fully chiral case) and the temperature is below a threshold ($T \leq 1/2$) we still see that only the symmetry-breaking phase exists in our model. Remarkably, this result shows that the chirality and the explicit breaking of the charge conjugation symmetry have a deep influence on the thermodynamic properties also in this infinite-range interacting context.

(q, φ)	$p = 1$	$p > 1$
$q = 3, \varphi \neq \frac{\pi}{q}$	1st order	1st order
$q = 3, \varphi = \frac{\pi}{q}$	No transition	No transition
$q > 3, \varphi \neq \frac{\pi}{q}$	2nd order	1st order
$q > 3, \varphi = \frac{\pi}{q}$	No transition	No transition

3. Free energy

In this section, we study the free-energy density $f(\beta, h)$ of the model at inverse temperature β in the thermodynamic limit, for a generic $q \geq 2$.

Thanks to the full connectivity of the interactions, a mean-field analysis provides a good description for the statistical-mechanical properties of the system. The canonical prescription for the mean-field

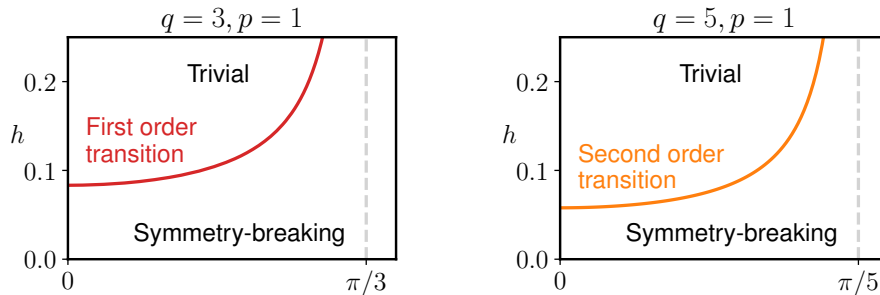


Figure 2. (Left panel) Phase diagram for the model with $q = 3$ and $p = 1$. Notice the first-order transition between symmetry-breaking and trivial phase and the phase-boundary tending to $h \rightarrow \infty$ for $\varphi \rightarrow \pi/3$. (Right panel) Phase diagram for $q = 5$ and $p = 1$. Now the transition is second order (a fact true for all $q > 3$) and at $\varphi = \pi/5$ the transition moves to infinity. For generic q this fact occurs at the fully chiral point $\varphi = \pi/q$.

approach on a quantum model involves first transforming the quantum partition function Z into a classical one by means of Suzuki-Trotter decomposition [27]. We introduce the order parameter, defined as $m = (|m|, \theta) = \langle \hat{m}_\sigma \rangle$, for the mean-field analysis and we apply the static approximation in order to remove the time dependence of the order parameter (see Appendix A for details). The free energy density of our model as calculated by this procedure is given by

$$f = (2p - 1)|m|^{2p} + f_s. \quad (10)$$

with

$$f_s = -\frac{1}{\beta} \log \text{Tr} e^{-\beta \hat{H}_s} \quad (11)$$

$$\hat{H}_s = -(\lambda^* \hat{\sigma} + \lambda \hat{\sigma}^\dagger) - hq^2(\hat{\tau} e^{i\varphi} + \hat{\tau}^\dagger e^{-i\varphi}). \quad (12)$$

where \hat{H}_s corresponds to a single-site Hamiltonian, and the complex number $\lambda = pm|m|^{2p-2}$ is an effective longitudinal field that depends on the average magnetization $m = \langle \hat{m}_\sigma \rangle$.

Computing the function f_s requires the diagonalization of a $q \times q$ Hermitian matrix. However, building on the Landau theory of phase transitions, general considerations can be formulated based on the symmetries of the model. As will become clear, we further need the assumption that f_s is an analytic function of λ and λ^* close to the point $\lambda = \lambda^* = 0$. In the following subsections we qualitatively discuss the expansion of the free energy density f_s as a power series in λ and λ^* , and we examine the case where the assumption of analyticity is not valid. In both cases, these arguments are sufficient to determine if a phase transition occurs and whether it can be continuous. Quantitative results concerning the expansion of the free energy density will be obtained using perturbation theory and are discussed in Section 4.

3.1. Series expansion

The single-site Hamiltonian Eq. (12) transforms under the unitary operator $\hat{\tau}$ and under time reversal \hat{T} as

$$\hat{\tau} \hat{H}_s(\lambda, \lambda^*) \hat{\tau}^\dagger = \hat{H}_s(\omega\lambda, \omega^*\lambda^*), \quad \hat{T} \hat{H}_s(\lambda, \lambda^*) \hat{T} = \hat{H}_s(\lambda^*, \lambda). \quad (13)$$

Since these transformations leave the trace of $\exp(-\beta \hat{H}_s)$ invariant, the free energy density f_s has to satisfy the following properties

$$f_s(\lambda, \lambda^*) = f_s(\omega\lambda, \omega^*\lambda^*), \quad f_s(\lambda, \lambda^*) = f_s(\lambda^*, \lambda). \quad (14)$$

As a consequence, the only non-zero terms that can appear in the power series are of the form $[\lambda^q + (\lambda^*)^q]^j (\lambda\lambda^*)^k$, for generic integers j, k . To lowest power in $|m|$ the free energy density f_s reads

$$f_s \simeq a_0 + a_2 \lambda \lambda^* = a_0 + a_2 p^2 |m|^{4p-2} \quad (15)$$

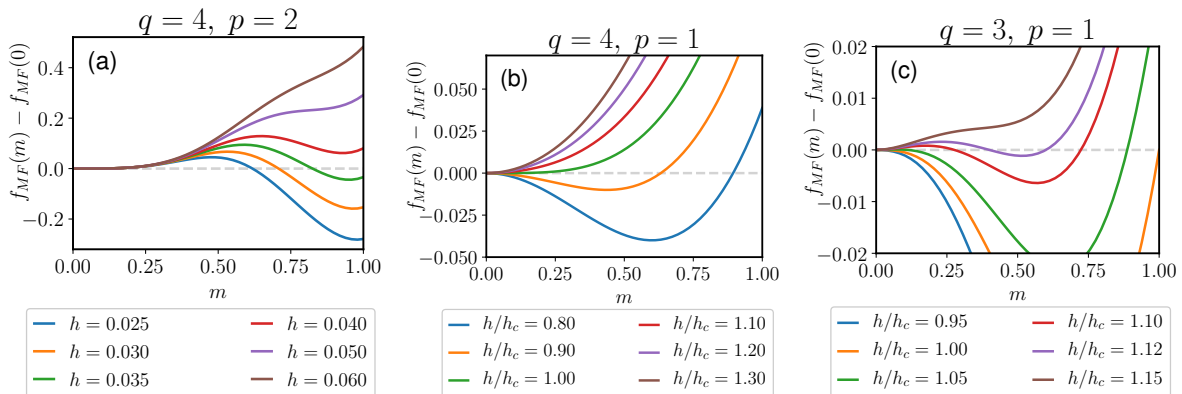


Figure 3. Free energy density at zero temperature as a function of m for $\varphi = 0$. (a) For $p > 1$ the transition from an ordered phase to a disordered one is of first order. (b) For $p = 1$, $q \geq 4$ the transition is of second order. (c) For $p = 1$, $q = 3$ the transition is of first order. The value of the field where the concavity in $m = 0$ changes sign is called h_c .

Using this relation in Eq. (10), we see that:

- For $p > 1$, the most relevant term in the limit $|m| \rightarrow 0$ is $(2p-1)|m|^{2p}$, which is always positive. This means that $m = 0$ is a local minimum, and the phase transition to an ordered phase with $|m| \neq 0$ can only be of first order (see Fig 3-a).
- For $p = 1$, on the other hand, the dominant term is $(1 + a_2)|m|^2$, so a continuous phase transition is in principle possible when $a_2 = -1$ (see Fig. 3-b). Another possibility is to have, as we vary h , a regime where $a_2 > -1$ (so $m = 0$ is locally a minimum) but a lower global minimum appears for $m \neq 0$ (see Fig. 3-c). We postpone to Section 4 a more detailed discussion about the order of the phase transition in this case.

3.2. Non-analytic behaviour

The results of the previous section crucially depend on the assumption that f_s is an analytic function of λ and λ^* close to the point $|\lambda| = 0$. We now show a case where this assumption is not valid (due to the chirality φ) and discuss the consequences on the properties of the phase transition.

Let us consider the case of $q > 2$ and zero temperature, for which f_s is equal to the ground state energy of \hat{H}_s , and examine how this energy depends on the small fields λ, λ^* . For $|\lambda| = 0$, $H_0 \equiv \hat{H}_s(\lambda = 0, \lambda^* = 0)$ is diagonal in the τ basis and has eigenvalues $-2hq^2 \cos(2\pi j/q + \varphi)$ for $j = 0, 1, \dots, q-1$. If the ground state of H_0 is unique (i.e. for $\varphi \neq \pi/q$), the first perturbative correction to the ground state energy is of second order (proportional to $\lambda\lambda^*$). On the other hand, if $\varphi = \pi/q$, the ground state of H_0 has double degeneracy. The Hamiltonian H_s restricted to the ground state manifold has the form

$$H_s|_{GS} = \begin{pmatrix} \epsilon_0 & -\lambda^* \\ -\lambda & \epsilon_0 \end{pmatrix} \quad (16)$$

with $\epsilon_0 = -2hq^2 \cos(\pi/q)$. We obtain that, to lowest order in $|\lambda|$, the ground state energy is $f_s \simeq \epsilon_0 - |\lambda|$, which is not an analytic function of λ and λ^* .

We deduce that, while the discussion of the previous section applies almost everywhere, a different scenario appears at zero temperature for $\varphi = \pi/q$. In this case, the free energy density in Eq. 10 reads

$$f = (2p-1)|m|^{2p} - 2hq^2 \cos(\pi/q) - p|m|^{2p-1} + O(|m|^{4p-2}/2hq^2). \quad (17)$$

Note that, in the limit of large h , we can neglect higher order terms, and the minimum is found for $|m| = 1/2$. Remarkably, the model does not have a transition to a paramagnet, and the magnetization remains finite for arbitrarily large field h . This peculiar behaviour is further discussed in Section 5.

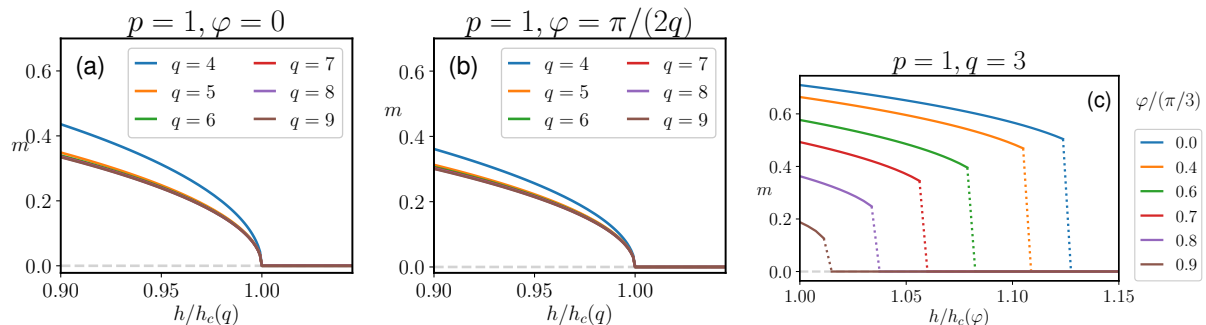


Figure 4. Magnetization m as a function of h/h_c (from Eq. 18). (a),(b) A second order phase transition occurs at $T = 0$, $h = h_c$ for different values of $q > 3$ and $\varphi < \pi/q$. (c) A first order phase transition takes place at $T = 0$, $h = h_* > h_c$ for $q = 3$ and different values of $\varphi < \pi/q$.

4. Continuous phase transition

Since a continuous phase transition has already been ruled out for $p > 1$, we will focus from now on on the case $p = 1$. As explained in the previous section, if a continuous phase transition occurs we can obtain the exact location in the phase diagram from the condition $a_2 = -1$. The coefficient a_2 can be computed exactly using perturbation theory, for arbitrary field h and inverse temperature β (explicit calculations are reported in Appendix B). In particular, as we show in Fig. 4-a and 4-b, the zero temperature transition is located at

$$h_c = \frac{1}{2q^2} \left[\left(\cos(\varphi) - \cos\left(\varphi + \frac{2\pi}{q}\right) \right)^{-1} + \left(\cos(\varphi) - \cos\left(\varphi - \frac{2\pi}{q}\right) \right)^{-1} \right], \quad (18)$$

while the transition at zero field occurs at $\beta_c = 1$.

There is, however, another possibility: the transition may be a discontinuous first-order one and may occur at a value of the field $h_* > h_c$ (or $\beta_* > \beta_c$). We argue that this is indeed the case for $q = 3$. In this case, the free energy density has a third order term $\propto 2|\lambda|^3 \cos(3\theta)$ which is negative for some values of $\theta = \arg(\lambda)$, and a fourth order term, which is always positive. Given these signs of the coefficients, it can be proven that for $h \rightarrow h_c^+$ the difference of the free energy densities $f_{MF}(m) - f_{MF}(0)$ becomes negative for certain values of m (see Appendix C). Therefore, $m = 0$ is not the global minimum: a first order phase transition occurs for a value $h_* > h_c$ (which we obtain numerically) at $T = 0$, as shown in Fig. 3-c and Fig. 4-c. For any other value of q , the third order coefficient is zero, and we expect the transition to be continuous (Fig. 4-a,b).

5. Case $\varphi = \pi/q$

From Eq. (18) we see that the zero-temperature critical field diverges when $\varphi \rightarrow \pi/q$. We have further proved in section 3.2 that no transition occurs for $\varphi = \pi/q$, in which case the magnetization tends to $m \rightarrow 1/2$ for $h \rightarrow \infty$. We illustrate this non-analytic behaviour in Fig. 5-a: both for a discontinuous and for a continuous transition, as we approach the value $\varphi = \pi/q$, the fields at the transition (h_* and h_c respectively) diverge. Moreover, for the discontinuous case, the jump of the magnetization at the transition (m_*) tends to zero. The asymptotic behaviours at $T = 0$ for $x = \pi/q - \varphi \ll 1$ read

$$h_c \simeq \frac{1}{4q^2 \sin(\pi/q)x} \quad (19)$$

and for $q = 3$

$$h_* \simeq h_c \left(1 + \frac{4}{3}x^2 \right) \quad m_* = 36h_*x^2. \quad (20)$$

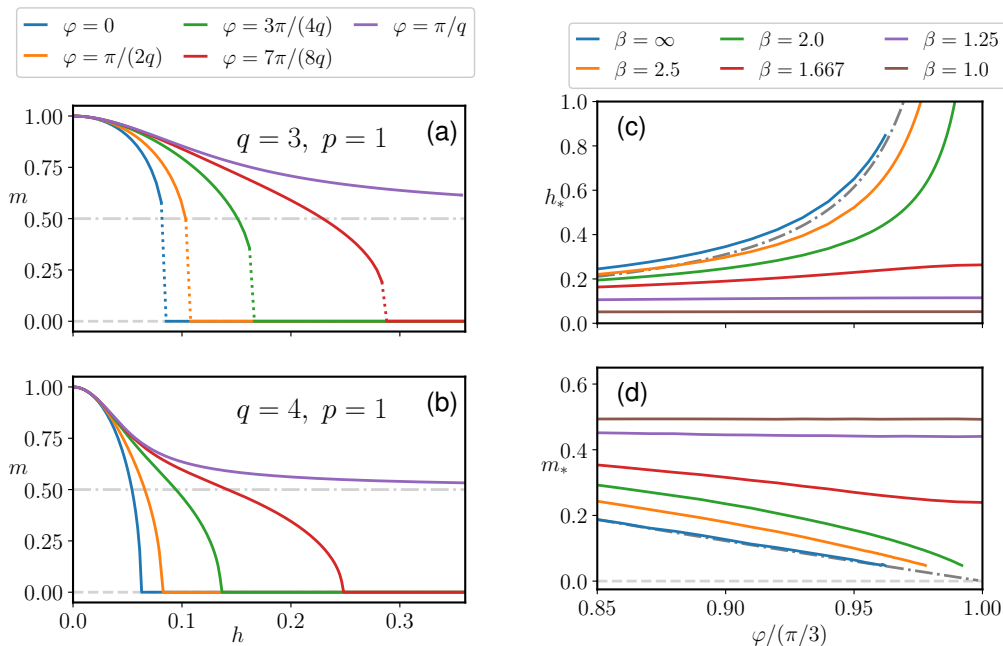


Figure 5. Magnetization m as a function of the field h for different values of φ in the cases (a) $q = 3, p = 1$ (first order transition) and (b) $q = 4, p = 1$ (second order transition). Field h_* (c) and magnetization m_* (d) at the discontinuous transition for $q = 3$ as a function of the chirality φ for different values of β .

As can be seen in Fig. 5-a, for $\varphi = \pi/q$, the magnetization is always larger than $1/2$.

We now consider the case of $T \neq 0$ but small compared to h , such that $h \cdot x \ll \beta^{-1} \ll h$. In this case, the perturbative expansion can be used and

$$a_2 \simeq -\frac{\tanh(2\beta h q^2 \sin(\pi/q)x)}{4h q^2 \sin(\pi/q)x} \simeq -\beta/2 \quad (21)$$

so if $\beta \geq 2$ for $p = 1$ the system is ferromagnetic in this regime. The phase transition can only occur out of this range, i.e. at a value of h diverging at least as fast as $1/x$. Since the transition point moves to $h \rightarrow \infty$ as $x \rightarrow 0$, we can argue that for $\beta \geq 2$, as already discussed in the zero-temperature case, when $\varphi = \pi/q$ ($x = 0$) the system is always ferromagnetic. This is in fact shown in Fig.5-b for $q = 3$, where a qualitative difference can be observed between $\beta \geq 2$ and $\beta < 2$. For $\beta \geq 2$ the transition point moves to diverging values of the field h_* when $x \rightarrow 0$, but it tends to a finite value when $\beta < 2$.

6. Large q limit

In this section, we derive an analytic expression for the free energy density at finite and zero temperature for large q . In this limit, the \mathbb{Z}_q symmetry of the model becomes a continuous $U(1)$ symmetry. The free energy density and the properties of the phase transition can be obtained from the spectrum of the single-site Hamiltonian \hat{H}_s , which now describes the dynamics of a continuous rotor. In order to take the continuum limit of the clock variable we replace

$$\sigma \rightarrow e^{i\alpha} \quad \tau \rightarrow e^{-\frac{2\pi}{q}\partial_\alpha} \quad (22)$$

such that τ acts on α as a translation of $2\pi/q$. With this substitution and by expanding τ to second order in the small parameter $2\pi/q$, we get

$$H_s = 4\pi^2 h \left(i \frac{\partial}{\partial \alpha} + \chi \right)^2 - 2|\lambda| \cos(\alpha + \theta) - 2hq^2 \quad (23)$$

where $\chi = q\varphi/(2\pi)$. Let us distinguish the cases $p = 1$ and $p > 1$. In the case $p = 1$, we have shown that, for any $q > 3$ the model has a second order phase transition at the critical value h_c in Eq. 18. Taking the limit $q \rightarrow \infty$ of this expression we find

$$h_c = \frac{1}{2\pi^2} \frac{1}{1 - 4\chi^2}. \quad (24)$$

On the other hand, for $p > 1$ the transition is first order and we use approximate methods for locating the transition point: we approximate the potential $-2|\lambda| \cos(\alpha + \theta)$ with a harmonic potential around $\alpha = -\theta$ and find the spectrum to be

$$E_n = -2|\lambda| - 2hq^2 + (4n + 2)\pi\sqrt{h|\lambda|}. \quad (25)$$

Using Eq. 10, we arrive at the following expression for the free energy density

$$f = (2p - 1) \left(\frac{|\lambda|}{p} \right)^{\frac{2p}{2p-1}} - 2hq^2 - 2|\lambda| + 2\pi q \sqrt{|\lambda|h} + -\frac{1}{\beta} \ln \left(\frac{\sinh(2\pi\beta\sqrt{|\lambda|h}q)}{\sinh(2\pi\beta\sqrt{|\lambda|h})} \right) \quad (26)$$

In the zero-temperature limit ($\beta \rightarrow \infty$), it follows from the principle of exponential dominance that the free energy density is given by $f = (2p - 1)|m|^{2p} + E_0$ for $\chi \neq 1/2$. In order to compute the magnetization (m_*) and field (h_*) at the transition, we need to solve two equations simultaneously. The first one is obtained by requiring the free energy of the paramagnet to be equal to the one of the ferromagnet at the transition point, *i.e.* $f(\lambda_*, \beta = \infty, h_*) = f(0, \beta = \infty, h_*)$. The second one is arrived at by minimizing the free energy with respect λ . The result is

$$h_* = \frac{2}{\pi^2} \frac{(2p)^{2p}}{(2p+1)^{2p+1}} \quad m_* = \frac{2p}{2p+1} \quad (27)$$

By requiring that the transition point belongs to the regime where the harmonic approximation is satisfied (*i.e.* $\sqrt{h|\lambda|} \ll |\lambda|$), we see that this result is valid when $p \gg 1$. In Fig. 6 we plot the numerical results for finite q and we see that, as expected, when we increase q they better approximate the analytical results in Eq. 27.

Similarly, the spinoidal field h_s and magnetization m_s are computed by solving two equations; the first obtained by requiring that $\frac{\partial^2 f}{\partial \lambda^2} = 0$ and second by minimizing the free energy density with respect to λ . We find that

$$h_s = \frac{32p^2}{\pi^2} \frac{(2p-1)^{2p-1}}{(6p-1)^{2p+1}} \quad m_s = \frac{2p-1}{6p-1}. \quad (28)$$

7. Conclusions and perspectives

We have examined the quantum and thermal properties of \mathbb{Z}_q -symmetric fully connected clock models, and classified the order of their phase transitions. We showed that the model can have first or second order phase transitions, which depend on the (i) chirality φ of the model, (ii) order p of the interactions, and (iii) dimensionality q of the clock variables. The full connectivity of the interactions has allowed us to solve the problem analytically by a combination of mean-field approach with perturbation theory up to fourth order.

In our analysis, we have first derived the free energy of the system in a mean-field level, which tends to be exact in the thermodynamic limit for fully connected models. In this way we have provided general considerations regarding the possible phase transitions that can occur in the model. We have applied a Landau-theory argument in the following way. We have expanded the free energy density in terms of the effective longitudinal field λ and examined it on the light of the symmetries of the model. In this way

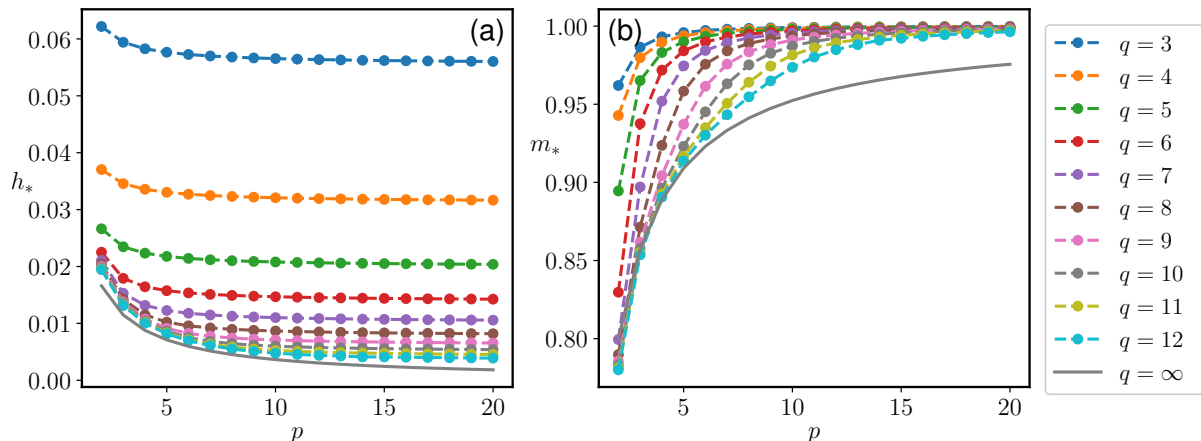


Figure 6. Values of the field h_* (panel (a)) and of the magnetization m_* (panel (b)) at the discontinuous phase transition for $p \geq 2$, and different values of q . The continuous line is the analytic result obtained in the large q limit (Eq. 27).

we have determined the possible phase transitions the model can have and their respective orders. The argument relies intimately on the condition that the free energy is an analytic function for small effective longitudinal fields, $\lambda \sim 0$. We have found that for $p > 1$ the possible phase transitions can only be of first order, while continuous transitions could in principle occur for $p = 1$.

The analyticity condition is satisfied almost always: In the case of a non-analytic free energy around $\lambda \sim 0$ the previous arguments do not apply. This is the case of the model at zero temperature with the specific chirality $\varphi = \pi/q$ and $q > 2$. In this case a different scenario appears and the model has no phase transition to a paramagnetic phase, independently of the value of p . Remarkably the magnetization remains finite for arbitrarily large fields h .

Using perturbation theory up to fourth order, we determined the coefficients of the free energy series expansion. This allowed us to perform a quantitative study of the phase transitions and delineate the phase diagram of the model for its different parameters p , q , φ and β .

In the limit $q \rightarrow \infty$ the \mathbb{Z}_q symmetry of the model becomes a continuous $U(1)$ symmetry. In this case we were able to go beyond perturbation theory results, and obtained analytically the free energy density of the model with its corresponding critical fields h_* and magnetization m_* (Eq.(27)), as well as its and spinodal fields h_s and magnetization m_s (Eq.(28)).

It is worth mentioning that our results are in agreement with previous works [21], where the case $p = 1$, $q = 3, 4$, $\varphi = 0$ was studied numerically. We remark that the phase structure in the case of infinite-range interactions is much simpler than the one of the one-dimensional short-range model, and has no incommensurate gapless phases. While in the short-range case for $q = 3$, $p = 1$ the transition between the trivial phase and the symmetry-breaking phase is second order, here the transition is first order. Also at $\varphi = \pi/3$ what we find is very different from the short-range case, which features a transition from a symmetry-breaking to an incommensurate phase [4]. The difference is evident also for larger q . For any $q > 3$, $p = 1$ in the infinite-range model there is a transition from symmetry-breaking to trivial phase but it is second order, in contrast with the already mentioned Kosterlitz-Thouless transition of the one-dimensional self-dual short-range case with $q > 4$. As a future perspective of this work, it would be interesting to extend the investigation to the case of long-range interactions in d dimensions, where it is possible to have some spatial dependence of correlations. This case interpolates between one-dimensional short-range and infinite-range cases; studying it would allow to understand the way one moves between two very different phase diagrams. In particular, this step would be important in order to understand what are the ingredients which allow for the presence of an incommensurate phase, like the one that arises in short-range interacting clock models in $d = 1$.

Acknowledgments

We acknowledge fruitful discussions with A. Angelone and M. Dalmonte. F.I. acknowledges the financial support of the Brazilian funding agencies CNPQ (308205/2019-7) and FAPERJ. This work is partly supported by the ERC under grant number 758329 (AGEnTh).

Bibliography

- [1] Eduardo Fradkin and Leo P. Kadanoff. Disorder variables and para-fermions in two-dimensional statistical mechanics. *Nuclear Physics B*, 170(1):1–15, 1980.
- [2] S. Ostlund. Incommensurate and commensurate phases in asymmetric clock models. *Phys. Rev. B*, 24:398–405, 1981.
- [3] G. Ortiz, E. Cobanera, and Z. Nussinov. Dualities and the phase diagram of the p -clock model. *Nucl. Phys. B*, 854:780, 2012.
- [4] Ye Zhuang, Hitesh J. Changlani, Norm M. Tubman, and Taylor L. Hughes. Phase diagram of the Z_3 parafermionic chain with chiral interactions. *Phys. Rev. B*, 92:035154, 2015.
- [5] Rhine Samajdar, Soonwon Choi, Hannes Pichler, Mikhail D. Lukin, and Subir Sachdev. Numerical study of the chiral F_3 quantum phase transition in one spatial dimension. *Phys. Rev. A*, 98:023614, 2018.
- [6] Seth Whitsitt, Rhine Samajdar, and Subir Sachdev. Quantum field theory for the chiral clock transition in one spatial dimension. *Phys. Rev. B*, 98:205118, 2018.
- [7] G. Sun, T. Vekua, E. Cobanera, and G. Ortiz. Phase transitions in the Z_p and $u(1)$ clock models. *Physical Review B*, 100:094428, 2019.
- [8] Paul Fendley. Parafermionic edge zero modes in zn-invariant spin chains. *Journal of Statistical Mechanics: Theory and Experiment*, 2012(11):P11020, 2012.
- [9] Chetan Nayak, Steven H. Simon, Ady Stern, Michael Freedman, and Sankar Das Sarma. Non-Abelian anyons and topological quantum computation. *Reviews of Modern Physics*, 80(3):1083–1159, 2008.
- [10] Paul Fendley. Free parafermions. *Journal of Physics A: Mathematical and Theoretical*, 47(7):75001, 2014.
- [11] Roberto Bondesan and Thomas Quella. Topological and symmetry broken phases of Z_N parafermions in one dimension. *Journal of Statistical Mechanics: Theory and Experiment*, 2013(10), 2013.
- [12] A Alexandradinata, N Regnault, Chen Fang, Matthew J Gilbert, and B Andrei Bernevig. Parafermionic phases with symmetry breaking and topological order. *Physical Review B*, 94(12), 2016.
- [13] Adam S Jermyn, Roger S.K. Mong, Jason Alicea, and Paul Fendley. Stability of zero modes in parafermion chains. *Physical Review B - Condensed Matter and Materials Physics*, 90(16), 2014.
- [14] David A. Huse. Simple three-state model with infinitely many phases. *Phys. Rev. B*, 24:5180–5194, 1981.
- [15] Steven Howes, Leo P Kadanoff, and Marcel Den Nijs. Quantum model for commensurate-incommensurate transitions. *Nuclear Physics B*, 215(2):169–208, 1983.
- [16] David A Huse, Anthony M Szpilka, and Michael E Fisher. Melting and wetting transitions in the three-state chiral clock model. *Physica A: Statistical Mechanics and its Applications*, 121(3):363–398, 1983.
- [17] Haruhiko Matsuo and Kiyohide Nomura. Berezinskii-Kosterlitz-Thouless transitions in the six-state clock model. *Journal of Physics A: Mathematical and General*, 39(12):2953–2964, 2006.
- [18] Natalia Chepiga and Frédéric Mila. Floating phase versus chiral transition in a 1d hard-boson model. *Phys. Rev. Lett.*, 122:017205, 2019.
- [19] G. Giudici, A. Angelone, G. Magnifico, Z. Zeng, G. Giudice, T. Mendes-Santos, and M. Dalmonte. Diagnosing potts criticality and two-stage melting in one-dimensional hard-core boson models. *Phys. Rev. B*, 99:094434, 2019.
- [20] Hannes Bernien, Sylvain Schwartz, Alexander Keesling, Harry Levine, Ahmed Omran, Hannes Pichler, Soonwon Choi, Alexander S Zibrov, Manuel Endres, Markus Greiner, et al. Probing many-body dynamics on a 51-atom quantum simulator. *Nature*, 551(7682):579, 2017.
- [21] Federica Maria Surace, Angelo Russomanno, Marcello Dalmonte, Alessandro Silva, Rosario Fazio, and Fernando Iemini. Floquet time crystals in clock models. *Phys. Rev. B*, 99:104303, 2019.
- [22] Angelo Russomanno, Simone Notarnicola, Federica Maria Surace, Rosario Fazio, Marcello Dalmonte, and Markus Heyl. Homogeneous floquet time crystal protected by gauge invariance. *Phys. Rev. Research*, 2:012003, 2020.
- [23] Victor Bapst and Guilhem Semerjian. On quantum mean-field models and their quantum annealing. *Journal of Statistical Mechanics: Theory and Experiment*, 2012(06):P06007, 2012.
- [24] Satoshi Morita and Hidetoshi Nishimori. Mathematical foundation of quantum annealing. *Journal of Mathematical Physics*, 49(12):125210, 2008.
- [25] T. Jörg, F. Krzakala, J. Kurchan, A. C. Maggs, and J. Pujos. Energy gaps in quantum first-order mean-field-like transitions: The problems that quantum annealing cannot solve. *EPL*, 89(4):40004, 2010.
- [26] Lov K. Grover. Quantum mechanics helps in searching for a needle in a haystack. *Phys. Rev. Lett.*, 79:325–328, 1997.
- [27] Masuo Suzuki. Generalized trotter’s formula and systematic approximants of exponential operators and inner derivations with applications to many-body problems. *Communications in Mathematical Physics*, 51(2):183–190, 1976.

Appendix A. Trotterization

Here we briefly outline the procedure for computing the Pseudo-free energy of our class of models. The partition function is given by

$$Z(\beta, h) = \text{Tr}[e^{-\beta H}] \quad (\text{A.1})$$

$$Z(\beta, h) = \sum_{\vec{\sigma}} \langle \vec{\sigma} | e^{\beta N(\hat{m}_\sigma \hat{m}_\sigma^\dagger)^p + \beta h q^2 N(e^{i\varphi} \hat{m}_\tau + e^{-i\varphi} \hat{m}_\tau^\dagger)} | \vec{\sigma} \rangle \quad (\text{A.2})$$

where $\vec{\sigma} = (\sigma_1, \dots, \sigma_n)$. The Suzuki-Trotter formula is used in order to map the system onto a classical model with an additional dimension α :

$$Z(\beta, h) = \lim_{N_s \rightarrow \infty} \sum_{\vec{\sigma}} \langle \vec{\sigma} | [e^{\beta N(\hat{m}_\sigma \hat{m}_\sigma^\dagger)^p / N_s} e^{\beta N h q^2 (e^{i\varphi} \hat{m}_\tau + e^{-i\varphi} \hat{m}_\tau^\dagger) / N_s}]^{N_s} | \vec{\sigma} \rangle \quad (\text{A.3})$$

We introduce N_s closure relations $\mathbf{1}(\alpha) = \sum_{\vec{\sigma}(\alpha)} |\vec{\sigma}(\alpha)\rangle \langle \vec{\sigma}(\alpha)|$
Where α indicates where the identity is sandwiched.

$$Z(\beta, h) = \lim_{N_s \rightarrow \infty} \sum_{\vec{\sigma}(1) \dots \vec{\sigma}(N_s)} \prod_{\alpha=1}^{N_s} \exp \left\{ \frac{\beta N}{N_s} \left[\left(\sum_{i=1}^N \frac{\sigma_i(\alpha)}{N} \right) \left(\sum_{i=1}^N \frac{\sigma_i(\alpha)^*}{N} \right) \right]^p \right\} \\ \times \langle \vec{\sigma}(\alpha) | e^{\beta N h q^2 [e^{i\varphi} \hat{m}_\tau + e^{-i\varphi} \hat{m}_\tau^\dagger] / N_s} | \vec{\sigma}(\alpha + 1) \rangle \quad (\text{A.4})$$

where $\sigma(N_s + 1) = \sigma(1)$. We apply N_s times the integral representation of the delta function
 $\int \delta(Nm_r(\alpha) - \Re[\sum_i \sigma_i]) \delta(Nm_{im}(\alpha) - \Im[\sum_i \sigma_i]) f(m_r, m_{im}) dm_{im} dm_r = f(\Re[\sum \frac{\sigma_i(\alpha)}{N}], \Im[\sum \frac{\sigma_i(\alpha)}{N}])$
where

$$\delta(Nm_{im}(\alpha) - \Im[\sum_i \sigma_i]) = \int_{-i\infty}^{i\infty} \frac{d\lambda_{im}}{\pi i N_s / (\beta N)} e^{-\frac{\beta}{N_s} 2\lambda_{im}(\alpha)(Nm_{im}(\alpha) - \Im[\sum_i \sigma_i(\alpha)])} \quad (\text{A.5})$$

$$\delta(Nm_r(\alpha) - \Re[\sum_i \sigma_i]) = \int_{-i\infty}^{i\infty} \frac{d\lambda_r e}{\pi i N_s / (\beta N)} e^{-\frac{\beta}{N_s} 2\lambda_r(\alpha)(Nm_r(\alpha) - \Re[\sum_i \sigma_i(\alpha)])} \quad (\text{A.6})$$

$$Z(\beta, h) = \lim_{N_s \rightarrow \infty} \int \frac{\prod_{\alpha} dm_{im}(\alpha) dm_r(\alpha) d\lambda_{im}(\alpha) d\lambda_r(\alpha)}{[\pi N_s / (\beta N)]^2} \quad (\text{A.7})$$

$$\exp \left[\frac{\beta N}{N_s} \left(\sum_{\alpha} (m_r^2(\alpha) + m_{im}^2(\alpha))^p - 2\lambda_r(\alpha)m_r(\alpha) - 2\lambda_{im}(\alpha)m_{im}(\alpha) \right) \right] \quad (\text{A.8})$$

$$\sum_{\vec{\sigma}(1) \dots \vec{\sigma}(N_s)} \prod_{\alpha} \langle \vec{\sigma}(\alpha) | e^{(\beta/N_s) \sum_i (h q^2 (e^{i\varphi} \tau_i + e^{-i\varphi} \tau_i^\dagger) + 2\lambda_{im}(\alpha) \Im[\sigma_i(\alpha)] + 2\lambda_{Re}(\alpha) \Re[\sigma_i(\alpha)])} | \vec{\sigma}(\alpha + 1) \rangle \quad (\text{A.9})$$

$$(\text{A.10})$$

where $2\lambda(\alpha)$ is the conjugate variable of the delta function. Using the fact that

$$\text{Tr}[A \otimes A \otimes \dots \otimes A] = (\text{Tr}[A])^n \quad (\text{A.11})$$

we transform the trace over all spins into that of a single-site problem

$$Z(\beta, h) = \lim_{N_s \rightarrow \infty} \int \frac{\prod_{\alpha} dm_{im}(\alpha) dm_r(\alpha) d\lambda_{im}(\alpha) d\lambda_r(\alpha)}{[\pi N_s / (\beta N)]^2} \quad (\text{A.12})$$

$$\exp \left[\frac{\beta N}{N_s} \left(\sum_{\alpha} (m_r^2(\alpha) + m_{im}^2(\alpha))^p - 2\lambda_r(\alpha)m_r(\alpha) - 2\lambda_{im}(\alpha)m_{im}(\alpha) \right) \right] \quad (\text{A.13})$$

$$+ \ln \left(\text{Tr} \prod_{\alpha} e^{\beta [h q^2 (e^{i\varphi} \tau + e^{-i\varphi} \tau^{\dagger}) - i\lambda_{im}(\alpha)(\sigma - \sigma^{\dagger}) + \lambda_{Re}(\alpha)(\sigma + \sigma^{\dagger})] / N_s} \right)^N \quad (\text{A.14})$$

Here we proceed with the static approximation by setting all the alphas to be equal.

$$Z(\beta, h) = \lim_{N_s \rightarrow \infty} \int \frac{dm_{im} dm_r d\lambda_{im} d\lambda_r}{[\pi N_s / (\beta N)]^2} \quad (\text{A.15})$$

$$\exp \left[\beta N \left((m_r^2 + m_{im}^2)^p - 2\lambda_r m_r - 2\lambda_{im} m_{im} \right) \right] \quad (\text{A.16})$$

$$+ \ln \left(\text{Tr} e^{\beta [h q^2 (e^{i\varphi} \tau + e^{-i\varphi} \tau^{\dagger}) - i\lambda_{im}(\sigma - \sigma^{\dagger}) + \lambda_{Re}(\sigma + \sigma^{\dagger})]} \right)^N \quad (\text{A.17})$$

The free energy density is given by the following formula

$$f(\beta, h) = -\frac{1}{\beta N} \ln Z \quad (\text{A.18})$$

and using the saddle point approximation our integral becomes

$$f(\beta, h) = \inf_{m_{im}, m_r} \text{ext}_{\lambda_{im}, \lambda_r} \left[-(m_r^2 + m_{im}^2)^p + \lambda_{im} m_{im} + \lambda_r m_r - \frac{1}{\beta} f_s(\beta, h, \lambda_{im}, \lambda_{re}, q) \right] \quad (\text{A.19})$$

where

$$f_s(\beta, h, \lambda_{im}, \lambda_{re}, q) = \ln \text{Tr} \left(e^{\beta [h q^2 (e^{i\varphi} \tau + e^{-i\varphi} \tau^{\dagger}) - i\lambda_{im}(\sigma - \sigma^{\dagger}) + \lambda_{Re}(\sigma + \sigma^{\dagger})]} \right) \quad (\text{A.20})$$

Taking partial derivatives of the f with respect to $\lambda_{im}, \lambda_{re}, m_{im}, m_{re}$ and setting the derivatives to be zero, we arrive at the following equations.

$$\lambda_{im} = m_{im} p (m_{im}^2 + m_{re}^2)^{p-1} \quad (\text{A.21})$$

$$\lambda_{re} = m_{re} p (m_{im}^2 + m_{re}^2)^{p-1} \quad (\text{A.22})$$

$$m_{im} = \frac{\partial f_s(\beta, h, \lambda_{im}, \lambda_{re}, q)}{2\beta \partial \lambda_{im}} \quad (\text{A.23})$$

$$m_{re} = \frac{\partial f_s(\beta, h, \lambda_{im}, \lambda_{re}, q)}{2\beta \partial \lambda_{re}} \quad (\text{A.24})$$

which can be written as

$$\vec{\lambda} = \vec{\nabla}_m |m|^{2p} \quad (\text{A.25})$$

$$\vec{m} = \frac{1}{\beta} \vec{\nabla}_{\lambda} g(\beta, h, \lambda_{im}, \lambda_{re}, q) \quad (\text{A.26})$$

$$(\text{A.27})$$

moving to radial coordinates we arrive at the following equations

let $\vec{\lambda} = (|\lambda|, \phi)$ and $\vec{m} = (|m|, \theta)$

$$|\lambda| = 2p|m|^{2p-1} \quad (\text{A.28})$$

$$\phi = \theta \quad (\text{A.29})$$

$$\theta = \frac{\partial g(\beta, h, \lambda, \phi, q)}{2\lambda\beta\partial\phi} \quad (\text{A.30})$$

$$|m| = \frac{\partial g(\beta, h, |\lambda|, q)}{2\beta\partial|\lambda|} \quad (\text{A.31})$$

Appendix B. Perturbation theory

In section 3.1 we showed that exploiting the symmetries of the model we can establish which terms can appear in the series expansion of the free energy density. In order to quantitatively determine the coefficients of the series expansion we resort to perturbative calculations. By defining

$$\hat{H}_0 = -hq^2(\hat{\tau}e^{i\varphi} + \hat{\tau}^\dagger e^{-i\varphi}), \quad \hat{V} = -(\lambda^*\hat{\sigma} + \lambda\hat{\sigma}^\dagger), \quad (\text{B.1})$$

the free energy density in Eq. (10) can be expressed as $f_s = \sum_{n=0}^{\infty} f_n$, with

$$f_0 = -\frac{1}{\beta} \log \text{Tr} e^{-\beta\hat{H}_0}, \quad f_n = -\frac{1}{\beta} \frac{(-1)^n}{n!} \int_0^\beta dt_1 \cdots \int_0^\beta dt_n \langle T[\hat{V}(t_1) \cdots \hat{V}(t_n)] \rangle_{0,c} \quad n \geq 1 \quad (\text{B.2})$$

where $\hat{V}(t) = e^{t\hat{H}_0}\hat{V}e^{-t\hat{H}_0}$, and $\langle T[\hat{V}(t_1) \cdots \hat{V}(t_n)] \rangle_{0,c}$ is the (imaginary-)time-ordered connected correlation function computed with respect to the unperturbed Hamiltonian \hat{H}_0 .

The expansion up to fourth order in the perturbation yields

$$f_s = a_0 + a_2\lambda\lambda^* + \delta_{q,2}c_2(\lambda^2 + (\lambda^*)^2) + \delta_{q,3}c_3(\lambda^3 + (\lambda^*)^3) + a_4\lambda^2(\lambda^*)^2 + \delta_{q,4}c_4(\lambda^4 + (\lambda^*)^4) + O(|\lambda|^5). \quad (\text{B.3})$$

We now want to find an expression for the coefficients a_n, c_n in terms of the unperturbed eigenvalues $\epsilon_i = -2hq^2 \cos(2\pi i/q + \varphi)$ and of $Z_0 = \sum_{i=0}^{q-1} e^{-\beta\epsilon_i}$.

Our goal is computing correlation functions of the following form

$$\int_0^\beta dt_1 \cdots \int_0^\beta dt_n \langle T[\hat{V}(t_1) \cdots \hat{V}(t_n)] \rangle_0 = n! \int_0^\beta dt_n \int_0^{t_n} dt_{n-1} \cdots \int_0^{t_2} dt_1 \langle \hat{V}(t_n) \cdots \hat{V}(t_1) \rangle_0. \quad (\text{B.4})$$

We denote by $|i\rangle$ and ϵ_i with $i = 0, \dots, q-1$ respectively the eigenstates of H_0 and the corresponding eigenvalues. Correlation functions can be computed inserting resolution of the identity $\sum_{i=0}^{q-1} |i\rangle \langle i|$ as follows

$$\langle \hat{V}(t_n) \cdots \hat{V}(t_1) \rangle_0 = \sum_{i_1=0}^{q-1} \cdots \sum_{i_n=0}^{q-1} e^{-\beta\epsilon_{i_n}} e^{t_n\epsilon_{i_n}} V_{i_n i_{n-1}} e^{-(t_n-t_{n-1})\epsilon_{i_{n-1}}} \cdots e^{-(t_2-t_1)\epsilon_{i_1}} V_{i_1 i_n} e^{-t_1\epsilon_{i_n}} \quad (\text{B.5})$$

where $V_{ij} = \langle i|\hat{V}|j\rangle$. Define $s_n = t_1 - t_n + \beta$ and $s_j = t_{j+1} - t_j$ for $j = 1, \dots, n-1$.

$$\begin{aligned} \int_0^\beta dt_n \int_0^{t_n} dt_{n-1} \cdots \int_0^{t_2} dt_1 \langle \hat{V}(t_n) \cdots \hat{V}(t_1) \rangle_0 &= \\ &= \frac{\beta}{nZ_0} \sum_{i_1=0}^{q-1} \cdots \sum_{i_n=0}^{q-1} \int_0^\beta \prod_{j=1}^n ds_j \delta\left(\sum_{j=1}^n s_j - \beta\right) V_{i_n i_{n-1}} \cdots V_{i_1, i_n} \prod_{j=1}^n e^{-s_j\epsilon_{i_j}} \end{aligned} \quad (\text{B.6})$$

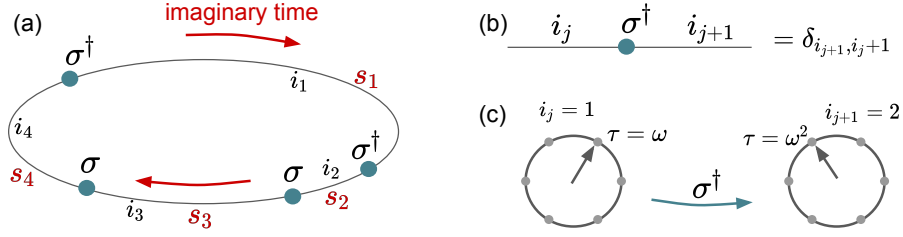


Figure B1. (a) Diagrammatic representation of the correlator $\langle \hat{\sigma}^\dagger(t_1)\sigma(t_2)\sigma(t_3)\hat{\sigma}^\dagger(t_4) \rangle_0$ computed as in Eq. (B.6). The loop in imaginary time has total length $\beta = s_1 + s_2 + s_3 + s_4$. The indices i_1, \dots, i_4 represent the virtual states over which the summation is performed. The green dots are the matrix elements. (b) The matrix elements of $\hat{\sigma}^\dagger$ in the τ representation are δ functions. (c) An example of two states i_j, i_{j+1} satisfying the condition $\langle i_{j+1} | \hat{\sigma}^\dagger | i_j \rangle = 1$.

Since $\hat{V} = \lambda\hat{\sigma} + \lambda^*\sigma^\dagger$, the last equation can be expressed as a sum of n -point correlators of the operators $\hat{\sigma}$ and σ^\dagger . Each correlator can be represented with a diagram as in Figure B1: each line represents the imaginary time evolution $e^{-s_j\epsilon_{i_j}}$ and the vertices σ and σ^\dagger flip the state i_j respectively to $i_j - 1$ and $i_j + 1$. Since the product couples also i_1 and i_n , it is easy to see that the only correlators which contribute are the ones where, at the end of the cycle, the state comes back to the original one. They correspond to the correlators with an equal number of σ and σ^\dagger , or the ones for which the difference between the numbers of σ and σ^\dagger operators is a multiple of q .

For each diagram we have to compute an integral of the form

$$I(\beta; \{E_j\}) = \int_0^\beta \prod_{j=1}^n ds_j \delta\left(\sum_{j=1}^n s_j - \beta\right) \prod_{j=1}^n e^{-s_j E_j} \quad (\text{B.7})$$

We Laplace transform and obtain

$$F(\kappa) = \int_0^{+\infty} d\beta e^{-\kappa\beta} I(\beta; \{E_j\}) = \int_0^{+\infty} \prod_{j=1}^n ds_j \prod_{j=1}^n e^{-s_j(\kappa + E_j)} = \prod_{j=1}^n (k + E_j)^{-1} \quad (\text{B.8})$$

in the region of convergence $\text{Re}(\kappa) > -E_{\min}$. We find $I(\beta; \{E_j\})$ as the inverse Laplace transform

$$I(\beta; \{E_j\}) = \frac{1}{2\pi i} \lim_{T \rightarrow +\infty} \int_{\gamma - iT}^{\gamma + iT} e^{\kappa\beta} \prod_{j=1}^n (k + E_j)^{-1} \quad (\text{B.9})$$

with $\gamma > -E_{\min}$. The integral is then easily computed using the residue theorem.

$$I(\beta; \{E_j\}) = \sum_j \text{Res}(f, -E_j) \quad (\text{B.10})$$

with $f(z) = e^{z\beta} \prod_{j=1}^n (z + E_j)^{-1}$ and the sum counts each pole once.

Appendix B.1. Order $n = 2$

For $q > 2$, it is easy to see that only two diagrams which contribute, and they give the same integral

$$\begin{aligned} \int_0^\beta dt_2 \int_0^{t_2} dt_1 \langle \hat{V}(t_2)\hat{V}(t_1) \rangle_0 &= |\lambda|^2 \left(\int_0^\beta dt_2 \int_0^{t_2} dt_1 \langle \hat{\sigma}(t_2)\hat{\sigma}^\dagger(t_1) \rangle_0 + \int_0^\beta dt_2 \int_0^{t_2} dt_1 \langle \hat{\sigma}^\dagger(t_2)\hat{\sigma}(t_1) \rangle_0 \right) \\ &= 2|\lambda|^2 \int_0^\beta dt_2 \int_0^{t_2} dt_1 \langle \hat{\sigma}(t_2)\hat{\sigma}^\dagger(t_1) \rangle_0 \quad (\text{B.11}) \end{aligned}$$

$$\int_0^\beta dt_2 \int_0^{t_2} dt_1 \langle \hat{\sigma}(t_2) \hat{\sigma}^\dagger(t_1) \rangle_0 = \frac{\beta}{2Z_0} \sum_{i=0}^{q-1} I(\beta; \epsilon_i, \epsilon_{i+1}) = -\frac{\beta}{2Z_0} \sum_{i=0}^{q-1} \frac{e^{-\beta\epsilon_{i+1}} - e^{-\beta\epsilon_i}}{\epsilon_{i+1} - \epsilon_i} \quad (\text{B.12})$$

The last equation is obtained for the case of simple poles. If, for some state i , $\epsilon_i = \epsilon_{i+1}$, the equation is valid with the substitution $\frac{e^{-\beta\epsilon_{i+1}} - e^{-\beta\epsilon_i}}{\epsilon_{i+1} - \epsilon_i} \rightarrow -\beta$.

The second order term in the expansion of the free energy is

$$f_2 = a_2 |\lambda|^2, \quad a_2 = \frac{1}{Z_0} \sum_{i=0}^{q-1} \frac{e^{-\beta\epsilon_{i+1}} - e^{-\beta\epsilon_i}}{\epsilon_{i+1} - \epsilon_i} < 0. \quad (\text{B.13})$$

Appendix B.2. Order $n = 3$

A third order term is present only for $q = 3$. In that case we get

$$\int_I dt \langle \hat{V}(t_3) \hat{V}(t_2) \hat{V}(t_1) \rangle_0 = \lambda^3 \int_I dt \langle \hat{\sigma}(t_3) \hat{\sigma}(t_2) \hat{\sigma}(t_1) \rangle_0 + (\lambda^*)^3 \int_I dt \langle \hat{\sigma}^\dagger(t_3) \hat{\sigma}^\dagger(t_2) \hat{\sigma}^\dagger(t_1) \rangle_0 \quad (\text{B.14})$$

where the notation $\int_I dt$ is used to denote the integration over the region $0 \leq t_1 \leq t_2 \leq t_3 \leq \beta$. We obtain

$$\int_I dt \langle \hat{\sigma}(t_3) \hat{\sigma}(t_2) \hat{\sigma}(t_1) \rangle_0 = \frac{\beta}{Z_0} I(\beta; \epsilon_0, \epsilon_1, \epsilon_2), \quad (\text{B.15})$$

$$I(\beta; \epsilon_0, \epsilon_1, \epsilon_2) = \frac{e^{-\beta\epsilon_0}}{(\epsilon_1 - \epsilon_0)(\epsilon_2 - \epsilon_0)} + \frac{e^{-\beta\epsilon_1}}{(\epsilon_2 - \epsilon_1)(\epsilon_0 - \epsilon_1)} + \frac{e^{-\beta\epsilon_2}}{(\epsilon_0 - \epsilon_2)(\epsilon_1 - \epsilon_2)}, \quad (\text{B.16})$$

from which we get the term of the free energy density

$$f_3 = c_3 \delta_{q,3} (\lambda^3 + (\lambda^*)^3), \quad c_3 = \frac{I(\beta; \epsilon_0, \epsilon_1, \epsilon_2)}{Z_0} \quad (\text{B.17})$$

Appendix B.3. Order $n = 4$

If $q \neq 4$, the only diagrams that contribute are

$$\begin{aligned} \int_I dt \langle \hat{V}(t_4) \hat{V}(t_3) \hat{V}(t_2) \hat{V}(t_1) \rangle_0 &= \\ &= 4|\lambda|^4 \int_I dt \langle \hat{\sigma}^\dagger(t_4) \hat{\sigma}^\dagger(t_3) \hat{\sigma}(t_2) \hat{\sigma}(t_1) \rangle_0 + 2|\lambda|^4 \int_I dt \langle \hat{\sigma}^\dagger(t_4) \hat{\sigma}(t_3) \hat{\sigma}^\dagger(t_2) \hat{\sigma}(t_1) \rangle_0 \end{aligned} \quad (\text{B.18})$$

(now the integration is over the region $0 \leq t_1 \leq t_2 \leq t_3 \leq t_4 \leq \beta$).

$$\int_I dt \langle \hat{\sigma}^\dagger(t_4) \hat{\sigma}^\dagger(t_3) \hat{\sigma}(t_2) \hat{\sigma}(t_1) \rangle_0 = \frac{\beta}{4Z_0} \sum_{i=0}^{q-1} I(\beta; \epsilon_{i-1}, \epsilon_i, \epsilon_{i+1}, \epsilon_i) \quad (\text{B.19})$$

$$\begin{aligned} I(\beta; \epsilon_{i-1}, \epsilon_i, \epsilon_{i+1}, \epsilon_i) &= \frac{\beta e^{-\beta\epsilon_i}}{(\epsilon_{i+1} - \epsilon_i)(\epsilon_{i-1} - \epsilon_i)} - \frac{e^{-\beta\epsilon_i}}{(\epsilon_{i+1} - \epsilon_i)(\epsilon_{i-1} - \epsilon_i)^2} - \frac{e^{-\beta\epsilon_i}}{(\epsilon_{i+1} - \epsilon_i)^2(\epsilon_{i-1} - \epsilon_i)} \\ &\quad + \frac{e^{-\beta\epsilon_{i+1}}}{(\epsilon_i - \epsilon_{i+1})^2(\epsilon_{i-1} - \epsilon_{i+1})} + \frac{e^{-\beta\epsilon_{i-1}}}{(\epsilon_i - \epsilon_{i-1})^2(\epsilon_{i+1} - \epsilon_{i-1})} \end{aligned} \quad (\text{B.20})$$

$$\int_I dt \langle \hat{\sigma}^\dagger(t_4) \hat{\sigma}(t_3) \hat{\sigma}^\dagger(t_2) \hat{\sigma}(t_1) \rangle_0 = \frac{\beta}{4Z_0} \sum_{i=0}^{q-1} I(\beta; \epsilon_{i+1}, \epsilon_i, \epsilon_{i+1}, \epsilon_i) \quad (\text{B.21})$$

$$I(\beta; \epsilon_{i+1}, \epsilon_i, \epsilon_{i+1}, \epsilon_i) = \frac{\beta(e^{-\beta\epsilon_i} + e^{-\beta\epsilon_{i+1}})}{(\epsilon_{i+1} - \epsilon_i)^2} + \frac{2(e^{-\beta\epsilon_{i+1}} - e^{-\beta\epsilon_i})}{(\epsilon_{i+1} - \epsilon_i)^3} \quad (\text{B.22})$$

For the case $q = 4$, there is an additional term coming from the diagram

$$\int_I dt \langle \hat{\sigma}(t_4) \hat{\sigma}(t_3) \hat{\sigma}(t_2) \hat{\sigma}(t_1) \rangle_0 = \frac{\beta}{Z_0} I(\beta; \epsilon_0, \epsilon_1, \epsilon_2, \epsilon_3). \quad (\text{B.23})$$

by inserting Eqs. B.11 and B.18 in

$$f_4 = -\frac{1}{4! \beta} \left[4! \int_I dt \langle \hat{V}(t_4) \hat{V}(t_3) \hat{V}(t_2) \hat{V}(t_1) \rangle_0 - 3 \cdot (2!)^2 \left(\int_0^\beta dt_2 \int_0^{t_2} dt_1 \langle \hat{V}(t_2) \hat{V}(t_1) \rangle_0 \right)^2 \right] \quad (\text{B.24})$$

and using Eqs. B.19, B.23 and B.12, we obtain the final result

$$f_4 = a_4 |\lambda|^4 + c_4 \delta_{q,4} (\lambda^4 + (\lambda^*)^4) \quad (\text{B.25})$$

with

$$a_4 = \frac{1}{2Z_0} \left[-\sum_{i=0}^{q-1} \left(2I(\beta; \epsilon_{i-1}, \epsilon_i, \epsilon_{i+1}, \epsilon_i) + I(\beta; \epsilon_{i+1}, \epsilon_i, \epsilon_{i+1}, \epsilon_i) \right) + \frac{\beta}{Z_0} \left(\sum_{i=0}^{q-1} I(\beta; \epsilon_i, \epsilon_{i+1}) \right)^2 \right], \quad (\text{B.26})$$

$$c_4 = -\frac{I(\beta; \epsilon_0, \epsilon_1, \epsilon_2, \epsilon_3)}{Z_0}. \quad (\text{B.27})$$

Appendix C. Proof of first order transition for $p = 1$, $q = 3$

We here prove that the transition is of the first order for $p = 1$, $q = 3$. Up to fourth order terms the free energy density has the form

$$f(\lambda \equiv |\lambda|e^{i\theta}) = C_0 + (1 + a_2)|\lambda|^2 + 2c_3 \cos(3\theta)|\lambda|^3 + a_4|\lambda|^4 + O(|\lambda|^6) \quad (\text{C.1})$$

where a_4 is positive for $h \simeq h_c$. The transition is first order if for a certain $a_2 > -1$ there exists some λ_* such that $f(\lambda_*) < f(0)$. Neglecting terms beyond fourth order, we find that this condition reduces to a second degree inequality, which has solutions only if

$$\Delta = (c_3 \cos(3\theta))^2 - a_4(1 + a_2) > 0 \quad (\text{C.2})$$

For $h \rightarrow h_c^+$ we have $(1 + a_2) \rightarrow 0^+$, so $\Delta > 0$ holds for h sufficiently close to h_c . We fix $\theta = 0$ if $c_3 < 0$ and $\theta = \pi/3$ if $c_3 > 0$, such that $2c_3 \cos(3\theta) = -2|c_3|$. Then, to lowest order in $1 + a_2$, the inequality is satisfied for

$$\frac{1 + a_2}{2|c_3|} < |\lambda| < \frac{2|c_3|}{a_4}. \quad (\text{C.3})$$

At this point one might be concerned that this solution may break when including terms beyond the fourth order. The crucial observation is that for $h \rightarrow h_c$, the lower extremum of the range in Eq. C.3 $(1 + a_2)/2|c_3|$ goes to 0: hence we find solutions for arbitrarily small values of $|\lambda|$, where higher order terms are negligible. Therefore, the existence of λ_* such that $f(\lambda_*) < f(0)$ can always be satisfied, for some $h > h_c$, and the transition is of the first order.